IEEE Access
Multidisciplinary | Rapid Review | Open Access Journal

Received November 27, 2018, accepted December 7, 2018, date of publication December 19, 2018,
date of current version January 11, 2019.

Digital Object Identifier 10.1109/ACCESS.2018.2887298

All Passive Realization of Lossy Coupling Matrices Using Resistive Decomposition Technique

RANJAN DAS[1], (Student Member, IEEE), QINGFENG ZHANG[1], (Senior Member, IEEE), ABHISHEK KANDWAL[2], (Member, IEEE), AND HAIWEN LIU[3], (Senior Member, IEEE)

[1]Department of Electronics and Electrical Engineering, Southern University of Science and Technology, Shenzhen 518055, China
[2]Shenzhen Institute of Advanced Technology, Chinese Academy of Sciences, Shenzhen 518055, China
[3]School of Electronic and Information Engineering, Xi'an Jiaotong University, Xi'an 710049, China

Corresponding author: Qingfeng Zhang (e-mail: zhang.qf@sustc.edu.cn)

This work was supported in part by the National Natural Science Foundation of China under Grant 61871207, in part by the Guangdong Natural Science Funds for Distinguished Young Scholar under Grant 2015A030306032, in part by the Talent Support Project of Guangdong under Grant 2016TQ03X839, and in part by the Shenzhen Science and Technology Innovation Committee funds under Grant KQJSCX20160226193445, Grant JCYJ20160301113918121, and Grant JSGG20160427105120572.

ABSTRACT A complex coupling matrix has been extensively used in lossy filters and negative group delay devices. For the realization, conventional technique decomposes the complex coupling matrix into lossy resonators and complex inverters. Since the complex inverter does not follow the passivity in some cases, the resultant realization may be globally passive but locally active. This paper proposes a new decomposition technique to ensure the passivity everywhere. It decomposes the complex coupling matrix into a resistive connection matrix and a conventional real coupling matrix, which are both passively realizable. This technique provides a passive realization of the complex coupling matrix. Furthermore, a loss equalization technique is also proposed, to further achieve a uniform quality factor (Q) distribution among all the lossy resonators. Several illustrative examples and an experimental validation are finally provided.

INDEX TERMS Lossy filter, complex coupling matrix, complex inverter, decomposition, resistive connection, quality factor.

I. INTRODUCTION

Microwave filters are important components in modern communication systems such as radar, cellular radio and satellite communications. Based on various applications, these filters are broadly classified into lossless and lossy filters. Lossless filters are useful for different cellular radio communication systems where very stringent requirements are followed in both base stations and receivers. Synthesis methods for such lossless filters are well developed and presented in many literatures [1]–[4]. Also, researcher proposes lossless filter design in bandpass domain [5] and more advanced filter design technique using LTCC technology [6]. To cope with modern communication system, tunable filter design were proposed in [2]. However all these methods are limited to lossless filters only. In practical, all lossless filters exhibit some amount of insertion loss and it becomes prominent for higher frequencies. Therefore, exact filter synthesis method should consider loss which is considered as more general case of filter design. Typically lossy filters are preferred in satellite communication systems which require high filtering performances. Depending upon system and position of the filter, high performance criteria also changes. For example, insertion loss and power handling criteria are critical parameters for output multiplexer (OMUX) filter banks in any satellite transponder. Therefore, dielectric or cavity filters are best choices for OMUX. On the other hand, in the receiver side, input multiplexer (IMUX) filter banks demand a very flat passband and sharp rejection in the passband edges, but the loss and power handling performances are secondary issues. To achieve a flat passband and sharp rejection, in addition to using high-quality resonators, adaptive pre-distortion techniques [7] did a good job. But such filters are always accompanied by nonreciprocal components such as isolators or circulators. Another common technique to achieve the flat passband and sharp transition is to use lower Q resonators to form a lossy filter, where the additional loss can be taken care by low-noise amplifiers (LNA) [8]. Lossy filters can be a potential solution for IMUX.

Synthesis method for lossy filter was firstly explored in [9] based on even and odd mode analysis. However, it was only

limited to symmetric networks. Lossy filter synthesis by pole-zero approximation based on solving nonlinear least square problem was discussed in [10] and [11] and demonstrated successfully in [12]. An exact synthesis technique based on uneven Q resonators was proposed in [13], where a sharp transition was achieved by absorbing rather than reflecting power. This technique brought in complex cross-couplings as a result of hyperbolic rotations in loss equalization. But it was limited to symmetric filters as well. Similarly, hyperbolic reflection was introduced in [14] as a complementary design tool for lossy filters instead of usual hyperbolic rotation. However both transformations result lossy outer resonators only. In [15] and [16], lossy coupling matrix synthesis technique was introduced to deal with both symmetric and asymmetric networks using coupled resonator based N+2 coupling matrix technique. Such lossy filters usually involve the operation of complex coupling matrices or lossy inverters. Lossy inverters with lumped components was introduced in [17]. But such designs were suffered from asymmetric responses specially for low order lossy filters. Design of microstrip lossy filter for satellite transponder was discussed in [18]. But such designs mostly suffered from large footprint and poor stop band performance. Recently substrate integrated waveguide (SIW) lossy filter with flat passband based on multiple dissipative cross-couplings was presented in [19] and [20] where sensitive slots were used to design lossy couplings. Also following the same technique it would be difficult to design higher order lossy filters due to its realization complexity. In an another recent work [21], double layer based conventional resistive cross couplings (RCC) was used to implement lossy filters. But complicated LCP bonded multilayer PCB technology was used for fabrication. Moreover filter performances were highly sensitive to multilayer cross-couplings and even for highly lossy filters it can lead to asymmetric passband response. Application of lossy microwave networks are not limited to filters only. Several superluminal networks were used to design based on synthesis of lossy coupled resonators. More recently, complex coupling matrix was also applied to the synthesis of negative group delay (NGD) devices [22]. Both lossy filters and NGD devices promote the advancement of complex coupling matrix.

Since the invention of complex coupling matrix, it has been a challenging task to realize and implement lossy couplings. The complex inverter has the same network architecture as the classic real inverter except that the inversion values (equal to the coupling coefficients) are complex. The major challenge of this realization lies in passive implementation of complex inverters.

In this paper, we come up with a rigorous passive realization technique for complex coupling matrix. Instead of using complex inverters, we regard series resistive connection as a new building block and directly extract it from the complex coupling matrix. Therefore, the complex coupling matrix is initially decomposed into a resistive connection matrix and a conventional real coupling matrix. Then both resistive connection matrix and real coupling matrix are realized passively. Major contributions of this work include: 1) locally passive realization of the complex coupling matrix is proposed in a rigorous manner; 2) resistive connection is extracted as an individual building block from the coupling matrix for the first time; 3) a loss equalization technique is also proposed for the realization of uniform Q distribution among all the resonators; 4) all passive realization of complex inverters are presented and discussed.

This paper is organized as follows. Sec. II briefly introduces how complex coupling matrix comes into view in lossy filter synthesis and subsequently reviews the conventional techniques to realize it. Sec. III discuss passive realization of a complex inverter using proposed modified block. Sec. IV elaborates CM decomposition technique with loss equalization strategy. Three numerical examples with an experimental validation are subsequently provided in Sec. V and Sec. VI, respectively. A conclusion is finally given in Sec. VII.

II. REVIEW ON COMPLEX COUPLING MATRIX

Before illustrating the proposed decomposition technique, we briefly introduce in this section how complex coupling matrix comes into view in lossy filter synthesis and subsequently review the conventional techniques to realize it, so that readers have a better understanding of the background. Here, the complex coupling includes both pure imaginary and general complex coupling.

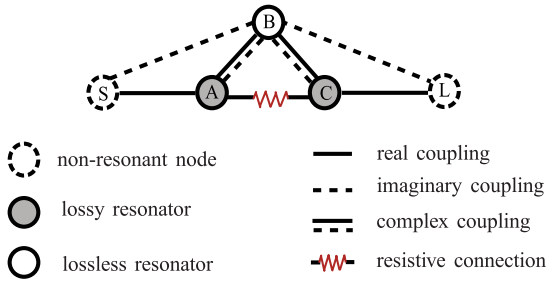

FIGURE 1. Illustration of all the symbols used in coupling topology throughout this paper.

Before going to any detail, we firstly illustrate in Fig. 1 all the coupling symbols used throughout this paper. Generally, we distinguish real coupling, imaginary coupling, complex coupling and resistive connection. Real coupling refers to the real coupling coefficient in coupling matrix, which is the same as the one used in lossless filters. Similarly, imaginary and complex coupling refer to pure imaginary and complex coupling coefficients, respectively. Further complex coupling coefficient refers to combination of both lossy and lossless couplings. Resistive connection is a new building block used in this paper, which represents a series resistor connected between two resonators. We emphasize here that resistive connection is different from *imaginary coupling* because they have different network parameters. This will be further explained in Sec. III. We will start with lossy filter synthesis technique to get better insight into lossy coupling matrix concept.

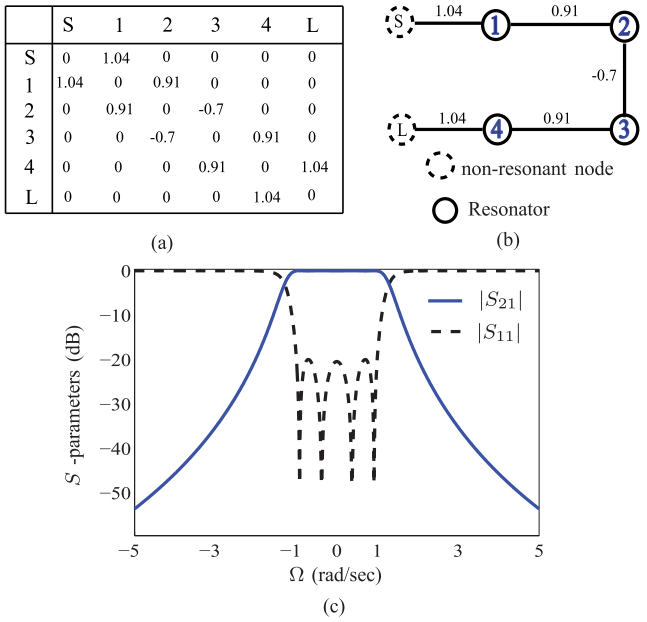

FIGURE 2. 4th-order lossless Chebyshev filter: (a) coupling matrix, (b) coupling topology, and (c) magnitude responses in low pass frequency domain.

A. LOSSY FILTER SYNTHESIS

Lossy filter design generally starts with synthesis of characteristic polynomials. The procedure is briefly introduced in [16]. It begins with a direct synthesis of lossless characteristic polynomials using the lossless filter design in [4]. Then, the lossy polynomials is obtained by a direct multiplication of both transmission and reflection polynomials by a constant attenuation factor, which preserve the polynomial and network orders. As shown in Fig. 2, let us consider a 4th-order Chebyshev filter used in [4]. Since the filter is lossless, the synthesized coupling matrix in Fig. 2(a) contains only conventional lossless (real) couplings and lossless resonators. Loss is subsequently incorporated by multiplying scattering polynomials with proper attenuation constant K_0 (=6 dB in this case). The corresponding lossy coupling matrix and coupling topology are depicted in Figs. 3(a) and (b), respectively. Note that, loss are concentrated at source and load nodes only while the inner resonators (2 and 3) are lossless, leading to a non-uniform Q_u distribution. Generally, it is preferable to distribute the loss equally among all the resonators for ease of implementation and fabrication. This is achieved by hyperbolic rotations as described in [13]. After loss equalization, the final resultant coupling matrix, coupling topology, and magnitude responses are presented in Figs. 3(c), (d), and Fig. 4, respectively. Note that, the coupling matrix contains several pure imaginary coupling (belonging to special case of complex coupling) between resonators. This is how complex coupling comes in the process of loss equalization. Note that two non-resonating nodes NS and NL (Fig. 3(d)) are introduced while loss distribution among resonators to avoid lossy S/L node as discussed in [16].

Let us consider another three-pole pseduoelliptic filter example. Following above lossy filter synthesis method,

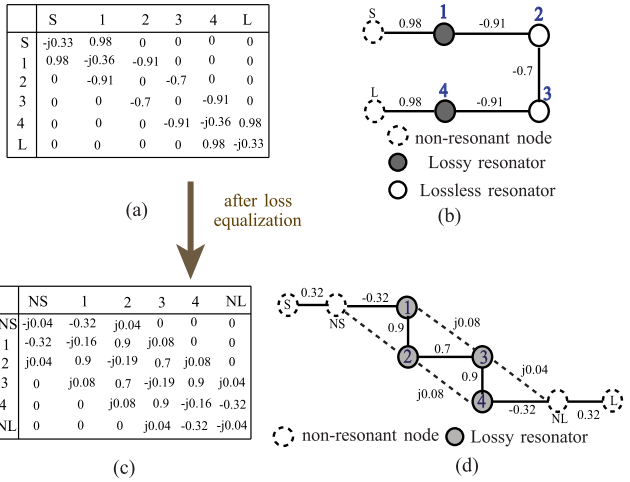

FIGURE 3. 4th-order lossy Chebyshev filter: (a) coupling matrix, (b) coupling topology before loss equalization, (c) coupling matrix, and (d) coupling topology after loss equalization with input/output coupling i.e. $M_{S,NS} = M_{L,NL} = 0.32$.

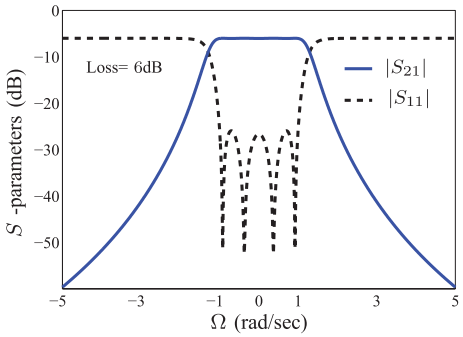

FIGURE 4. Magnitude responses of the lossy filter in Fig. 3.

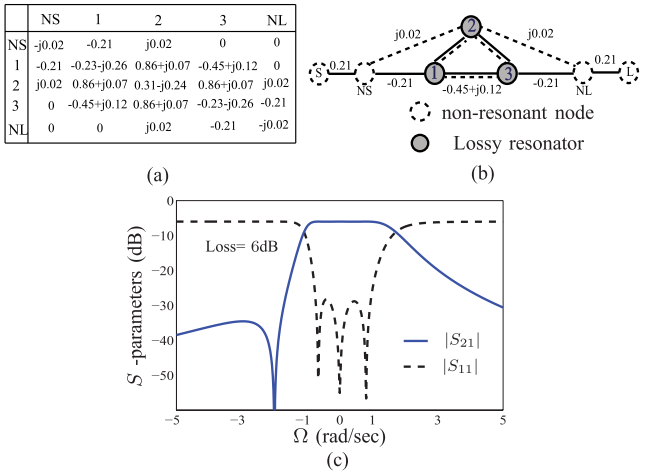

FIGURE 5. Loss equalized 3rd-order asymmetric pseduoelliptic filter: (a) coupling matrix with input/ouput coupling i.e. $M_{S,NS} = M_{L,NL} = 0.21$, (b) coupling topology, and (c) magnitude responses.

the final coupling matrix, coupling topology and magnitude responses are depicted in Fig. 5. Note that, the coupling matrix includes real, pure imaginary and complex

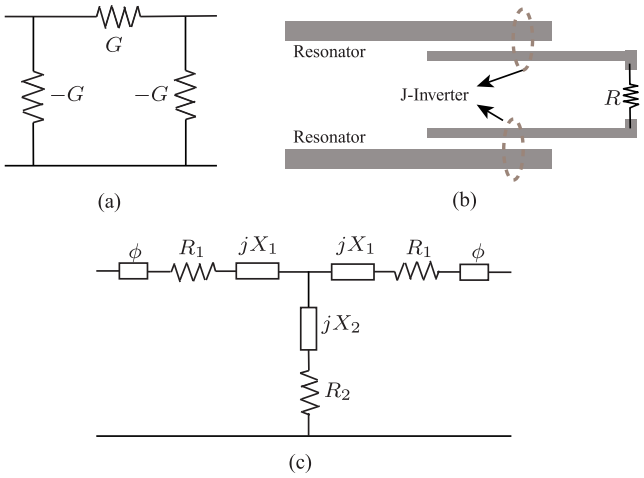

FIGURE 6. (a) Equivalent network and (b) implementation of an imaginary inverter, and (c) network realization of a complex inverter in [16].

coupling coefficients. This example represents a more general coupling matrix configuration.

It is important to mention that there exist an alternative technique to synthesize lossy filters based on even Q coupled resonators as described in [10]–[12]. This method rely on pole-zero approximation based on the solution of a nonlinear least squares problem. In summary, all the existing lossy filter synthesis techniques deal with multiple lossy cross-couplings along with conventional lossless couplings.

The above two examples illustrate how complex coupling comes into view and plays important role in lossy filter synthesis. It comes as the result of loss equalization in lossy filters. The recent work on coupling matrix synthesis of negative group delay devices [22] belongs to the other case where complex coupling directly comes into the coupling matrix without performing any loss equalization technique. In summary, complex coupling matrix is an inevitable synthesis outcome for both lossy filters and negative group delay devices. Now, we will briefly discuss in the next subsection the conventional realization techniques for such complex coupling matrices.

B. REALIZATION OF COMPLEX COUPLING MATRIX

For the realization, the classic technique, e.g. [16], decomposed the complex coupling matrix of Fig. 3(c) into coupling parts and lossy resonators. The coupling parts, including both imaginary (lossy) and real (lossless) coupling, are realized by inverters. The imaginary inverter has the admittance matrix as:

$$[Y]_{imaginary} = \begin{bmatrix} 0 & -G \\ -G & 0 \end{bmatrix}, \tag{1}$$

where G is a real value related to the coupling coefficient M by $M = jG$. The equivalent network of (1) and its classic implementation are shown in Figs. 6(a) and (b), respectively. Presence of negative shunt admittances in Fig. 6(a) makes it difficult to realize using passive components only. A passive implementation technique is described in [16] as shown in Fig. 6(b). However it is not rigorously equivalent to Fig. 6(a) and (1). For hybrid network realization of complex inverters as shown in Fig. 6(c), one has to deal with similar issues.

In summary, the conventional technique involves non-passive or inexact realization. We will propose a new passive fundamental block to deal with complex inverter implementation issue in next section.

III. MODIFIED BLOCK

The admittance matrix $[Y]$ of a general J-inverter is expressed as

$$[Y] = \begin{bmatrix} 0 & jJY_0 \\ jJY_0 & 0 \end{bmatrix}, \tag{2}$$

where J equals to the coupling coefficient which can be a complex or real quantity, and Y_0 is the characteristics admittance of the port.

Let us further consider two special cases. In one case, J is real then all elements in admittance matrix $[Y]$ become reactive. Thus, a real inverter is always passive and lossless. This also explains why real inverters are useful in filter design. In contrast, all elements in admittance matrix $[Y]$ will be real when J is pure imaginary. Thus, an imaginary inverter is always lossy.

Here, we slightly modify the conventional admittance matrix in (2) of a imaginary inverter to make it completely passive. The admittance matrix of the modified block is

$$[Y]_{\text{mod}} = Y_0 \begin{bmatrix} G_1 & -J_i \\ -J_i & G_2 \end{bmatrix}, \tag{3}$$

where G_1 and G_2 are two new real quantities in addition to the original imaginary inverter, J_i is a positive real quantity. Equivalent circuit model is presented in Fig. 7(a). One can conclude from Fig. 7(a) that all the components are passive when $G_1 \geq J_i$ and $G_2 \geq J_i$.

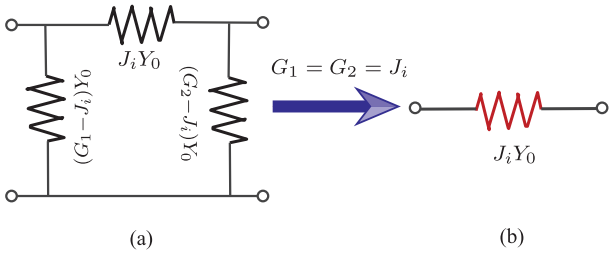

FIGURE 7. (a) Equivalent circuit model of the modified circuit block in (3), and (b) its reduction to a series resistive connection at $G_1 = G_2 = J_i$.

Consider a special case when $G_1 = G_2 = J_i$. The admittance parameters of the two shunt components in Fig. 7(a) become zero, and thus the equivalent network reduces to a series resistor as shown in Fig. 7(b). The resultant admittance matrix reads

$$[Y]_{\text{resistor}} = Y_0 \begin{bmatrix} J_i & -J_i \\ -J_i & J_i \end{bmatrix} \tag{4}$$

Instead of imaginary inverter, one may use this resistive connection in (4) as a new building block in the decomposition of complex coupling matrix. The coupling matrix form for this resistive connection will be

$$[M]_{\text{resistor}} = \begin{bmatrix} -jJ_i & jJ_i \\ jJ_i & -jJ_i \end{bmatrix} \tag{5}$$

One may extract this block directly from the complex coupling matrix using the decomposition technique as illustrated in the following section. Previously non-ideal inverter building block was discussed in [23] as series or shunt stub to introduce a controllable frequency-dependent coupling between microwave resonators. But here we will be used (4) as fundamental building block for passive realization of lossy cross-couplings.

One should also note that this resistive connection is considered as the special case of the modified block in (3). It is always passive. One also has other different forms depending on the choices of G_1 and G_2. Here, we only consider the resistive connection (4) for simplicity.

IV. COUPLING MATRIX DECOMPOSITION

A. RESISTIVE CONNECTION EXTRACTION

In the conventional technique, one decomposes all the complex off-diagonal entries into real and imaginary parts, where each imaginary part form a imaginary sub-matrix, and the rest form a single conventional matrix, i.e.

$$[M]_{\text{complex}} = [M]_{\text{conv}} + \sum_{n=1}^{N} [M]^n_{\text{imag}}, \tag{6}$$

where $[M]_{\text{conv}}$ is the same as the conventional coupling matrix where all the off-diagonal entries are real, $[M]^n_{\text{imag}}$ represents the n^{th} imaginary coupling, and N is the total number of imaginary coupling. Consider a second-order example,

$$\begin{bmatrix} -0.2-j0.2 & -0.4+j0.1 \\ -0.4+j0.1 & -0.2-j0.2 \end{bmatrix} = \begin{bmatrix} -0.2-j0.2 & -0.4 \\ -0.4 & -0.2-j0.2 \end{bmatrix} + \begin{bmatrix} 0 & j0.1 \\ j0.1 & 0 \end{bmatrix}. \tag{7}$$

Note that the second part of (7) is an imaginary inverter which is typically implemented using any one form as depicted in Fig. 6.

To make all the components passive, we reformulate the decomposition as

$$[M]_{\text{complex}} = [M]'_{\text{conv}} + \sum_{n=1}^{N} [M]^n_{\text{resistor}}, \tag{8}$$

where $[M]^n_{\text{resistor}}$ represents a resistive connection having the same form as (5), $[M]'_{\text{conv}}$ is a reformulated matrix different from $[M]_{\text{conv}}$ of (8). To illustrate this decomposition, consider a complex sub-matrix formed by k^{th} and l^{th} resonators, as shown in (9), as shown at the bottom of this page. Note that, the second part of (9) is a resistive connection between k^{th} and l^{th} resonators. If taking (7) as the example, one has the decomposition

$$\begin{bmatrix} -0.2-j0.2 & -0.4+j0.1 \\ -0.4+j0.1 & -0.2-j0.2 \end{bmatrix} = \begin{bmatrix} -0.2-j0.1 & -0.4 \\ -0.4 & -0.2-j0.1 \end{bmatrix} + \begin{bmatrix} -j0.1 & j0.1 \\ j0.1 & -j0.1 \end{bmatrix}. \tag{10}$$

Note that, the two parts of (10) are passive. The first part represents two lossy resonators coupled by a real inverter, which is implemented using conventional technologies. The second part is the proposed resistive connection block (5).

In summary, by applying the decomposition technique in (8) and (9), the complex coupling matrix is divided into a conventional coupling matrix $[M]'_{\text{conv}}$ plus several resistive connection sub-matrices $[M]^n_{\text{resistor}}$. One may combine all the resistive connection sub-matrices into a single matrix $[M]_{\text{resistor}}$, namely resistive connection matrix, representing the resistive connection information of all the resonators. In the implementation, one firstly employs the conventional technique to implement $[M]'_{\text{conv}}$, and subsequently connects resistors between resonators following $[M]_{\text{resistor}}$. This decomposition guarantees that all the sub-components are passive, and thus one is able to compare each implemented sub-component with its ideal circuit counterpart. The overall procedure is mathematically and physically rigorous. It is important to note that proposed CM decomposition (8) is different from typical decomposition (6), as proposed method always ensure $[M]_{\text{resistor}}$ will be set of series resistors connected between resonators.

This new approach of CM decomposition is extremely useful for lossy filter design and tuning. Firstly, it decomposes whole network as lossy part and lossless part which can be designed simultaneously. Thus it offers an efficient and fast design approach. Secondly, one-to-one correspondence between design parameters and coupling matrix elements reduces the optimization time significantly. Above all simple passive realization of lossy sub-coupling matrices as series resistor blocks, make the design and tuning method superior as compare to all other existing techniques. Recently, such CM decomposition based fast tuning algorithm for lossy

$$\begin{array}{c} \\ \vdots \\ k \\ \vdots \\ l \\ \vdots \end{array} \begin{array}{c} \cdots \quad k \quad \cdots \quad l \quad \cdots \\ \begin{bmatrix} \ddots & & & & \\ & \alpha_1 - j\beta_1 & \cdots & \alpha + j\beta & \\ & \vdots & \ddots & \vdots & \\ & \alpha + j\beta & & \alpha_2 - j\beta_2 & \\ & & & & \ddots \end{bmatrix} \end{array} = \begin{array}{c} \\ \vdots \\ k \\ \vdots \\ l \\ \vdots \end{array} \begin{array}{c} \cdots \quad k \quad \cdots \quad l \quad \cdots \\ \begin{bmatrix} \ddots & & & & \\ & \alpha_1 - j(\beta_1 - \beta) & \cdots & \alpha & \\ & \vdots & \ddots & \vdots & \\ & \alpha & & \alpha_2 - j(\beta_2 - \beta) & \\ & & & & \ddots \end{bmatrix} \end{array} + \begin{array}{c} \\ \vdots \\ k \\ \vdots \\ l \\ \vdots \end{array} \begin{array}{c} \cdots \quad k \quad \cdots \quad l \quad \cdots \\ \begin{bmatrix} \ddots & & & & \\ & -j\beta & \cdots & j\beta & \\ & \vdots & \ddots & \vdots & \\ & j\beta & & -j\beta & \\ & & & & \ddots \end{bmatrix} \end{array} \tag{9}$$

filters were discussed in [24] to prove the robustness and extended application of this new technique.

B. LOSS EQUALIZATION STRATEGY

As indicated by (9), the extraction of resistive connection matrix $[M]_{\text{resistor}}$ changes the imaginary parts of diagonal entries in the residual matrix $[M]'_{\text{conv}}$. Since the imaginary part of the diagonal entry represents the loss or unloaded quality factor (Q_u) of each resonator, this extraction procedure leads to a nonuniform Q_u distribution in $[M]'_{\text{conv}}$ if the original complex coupling matrix has a uniform Q_u distribution. For implementation convenience, one usually prefers a uniform Q_u distribution in $[M]'_{\text{conv}}$. Therefore, one should consider this decomposition effect when applying the hyperbolic rotation to the original complex coupling matrix.

Here, we propose a new loss equalization technique that combines the hyperbolic rotation and decomposition effect. Firstly, one specifies Δ as the final imaginary part of all the diagonal entries in $[M]'_{\text{conv}}$. Then, when applying hyperbolic rotation to k_{th} resonator, one enforces the following condition

$$\Im\left[R_h(M)_{kk} - \sum_{l=1,l\neq k}^{L} R_h(M)_{kl}\right] = \Delta, \qquad (11)$$

where $R_h(.)$ is the hyperbolic rotation of the matrix M, $\Im[.]$ is the operation of taking the imaginary part. To do this, the parameter of the hyperbolic rotation $R_h(.)$ is optimized to satisfy (11). Note that here we used hyperbolic rotation to distribute losses equally among resonators but it is possible to achieve the same results by using hyperbolic reflection operator as described in [14].

To summarize the whole design procedure for a lossy filter, we provide a design flow chart in Fig. 8.

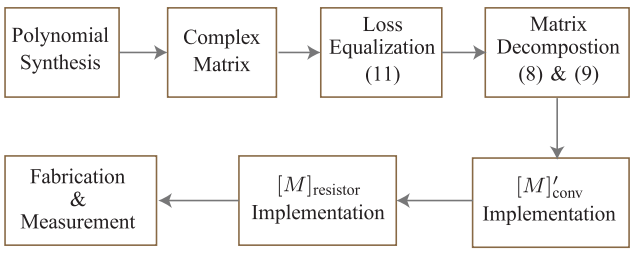

FIGURE 8. Flow chart of a lossy filter design incorporating the proposed decomposition and loss equalization techniques.

V. ILLUSTRATIVE EXAMPLES

To illustrate and validate the proposed decomposition technique and loss equalization strategy, three lossy filters are designed. Without loss of generality, both pure imaginary coupling and complex coupling cases are presented, both symmetrical and asymmetrical responses are considered, and both even-order and odd-order filters are designed.

A. EXAMPLE I: 4th-ORDER CHEBYSHEV FILTER

The first example is a 4$^{\text{th}}$-order Chebyshev lossy filter with 8.5 dB insertion loss and 28.5 dB return loss. The synthesized

TABLE 1. Synthesized polynomials of example I.

$E(s)$	$s^4 + 2.1436s^3 + 3.2974s^2 + 2.8281s + 1.25$
$P(s)$	$j0.463$
$F_{11}(s) = F_{22}(s)$	$0.370s^4 + 0.370s^2 + 0.046$

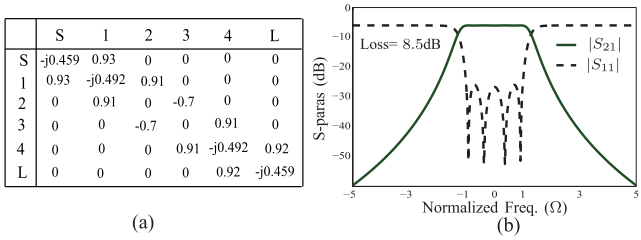

FIGURE 9. (a) Coupling matrix and (b) magnitude responses of example I before loss equalization.

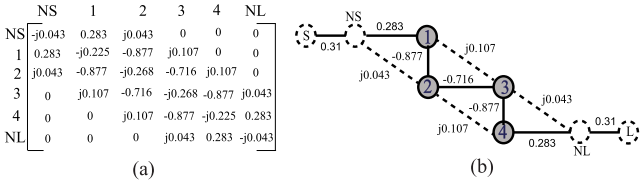

FIGURE 10. (a) Coupling matrix and (b) topology of example I after loss equalization with input/output couplings of $M_{S,NS} = M_{L,NL} = 0.303$.

polynomials, coupling matrix and magnitude responses are shown in Tab. 1 and Fig. 9, respectively. Note from Fig. 9(a) that the loss are mainly distributed in source, load, 1$^{\text{st}}$ and 4$^{\text{th}}$ resonators. After loss equalization using the proposed technique in Sec. IV-B, the complex coupling matrix and topology are shown in Fig. 10. Note that, the loss is equalized among all the resonators, and as a result, four imaginary coupling coefficients appear in the coupling matrix. One subsequently applies the proposed decomposition technique to the complex coupling matrix in Fig. 10(a), leading to four sub-matrices corresponding to four resistive connections, as shown in Fig. 11, and one residue matrix corresponding to the conventional coupling matrix without complex coupling values, as shown in Fig. 12(a). As expected, the residue coupling matrix has a uniform loss distribution among all the resonators. All the resistive connection sub-matrices are further combined together to form a single resistive connection matrix and topology, as shown in Fig. 12(b). Therefore, after the decomposition, one has two matrices in Fig. 12, one corresponding to the conventional coupling matrix and the other corresponding to the resistive connection matrix.

B. EXAMPLE II: 4th-ORDER QUASI-ELLIPTIC FILTER

The second example is a 4$^{\text{th}}$-order quasi-elliptic lossy filter with 7 dB insertion loss, 32 dB return loss, and two transmission zeros at $\Omega = \pm 2$. The synthesized polynomials, coupling matrix and magnitude responses are shown in Tab. 2 and Fig. 13, respectively. After loss equalization, the

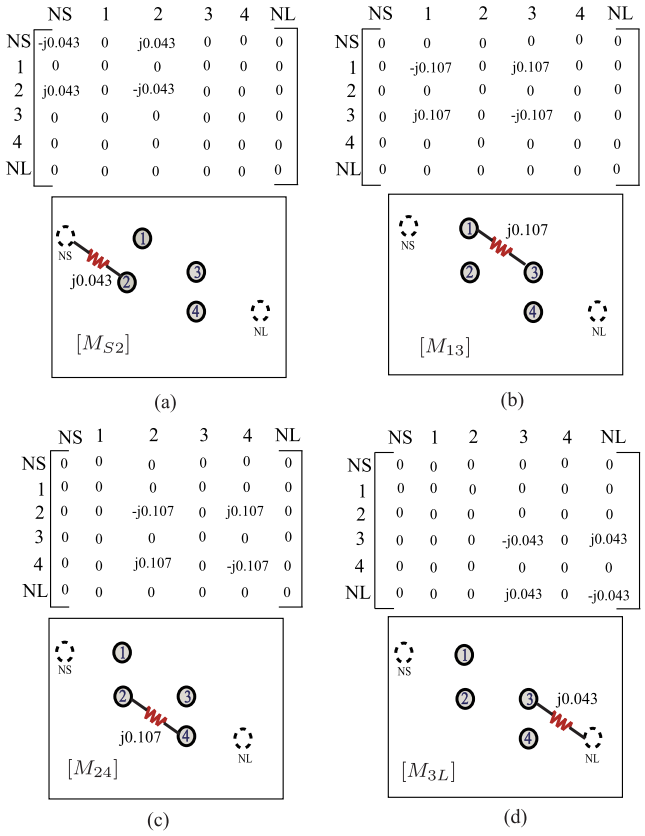

FIGURE 11. Four resistive connection sub-matrices decomposed from the complex coupling matrix of Fig. 10(a).

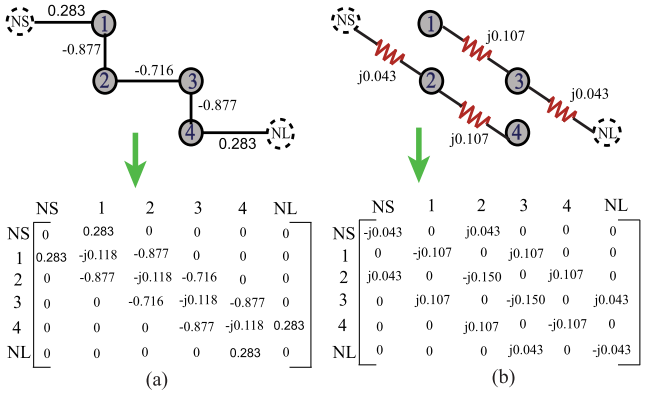

FIGURE 12. (a) Residue coupling matrix $[M]_{conv}$ and (b) resistive connection matrix $[M]_{resistor}$ after the decomposition of Fig. 10(a).

TABLE 2. Synthesized polynomials of example II.

$E(s)$	$s^4 + 2.5175s^3 + 4.3414s^2 + 4.315s + 2.5524$
$P(s)$	$j0.2838s^2 + j1.134$
$F_{11}(s) = F_{22}(s)$	$0.445s^4 + 0.461s^2 + 0.063$

complex coupling matrix and topology are shown in Fig. 14. Note that, the loss is equalized among all the resonators, and as a result, four imaginary coupling coefficients appear

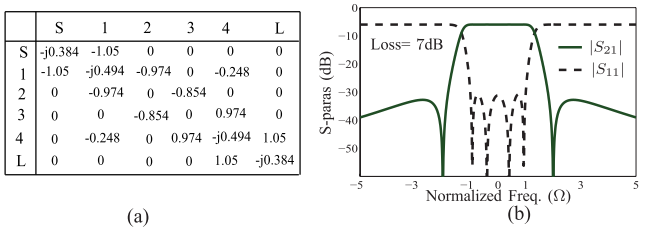

FIGURE 13. (a) Coupling matrix, and (b) magnitude responses of example II before loss equalization.

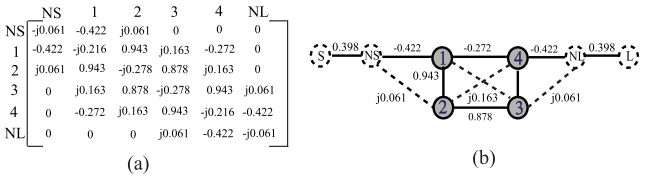

FIGURE 14. (a) Coupling matrix, and (b) topology of example II after loss equalization with input/output couplings of $M_{S,NS} = M_{L,NL} = 0.398$.

in the coupling matrix. One subsequently applies the proposed decomposition technique to the complex coupling matrix in Fig. 14(a), leading to four sub-matrices corresponding to four resistive connections, as shown in Fig. 15, and one residue matrix corresponding to the conventional coupling matrix without complex coupling values, as shown in Fig. 16(a). As expected, the residue coupling matrix has a uniform loss distribution among all the resonators. All the resistive connection sub-matrices are further combined together to form a single resistive connection matrix and topology, as shown in Fig. 16(b). Finally, one has two matrices in Fig. 16, one corresponding to the conventional coupling matrix and the other corresponding to the resistive connection matrix.

C. EXAMPLE III: 3rd-ORDER FILTER WITH ASYMMETRICAL REsponse

The third example is a 3rd-order quasi-elliptic lossy filter with 6 dB insertion loss, 28 dB return loss, and one transmission zero at $\Omega = -2$. The synthesized polynomials, coupling matrix and magnitude responses are shown in Tab. 3 and Fig. 17, respectively. After loss equalization, the complex coupling matrix and topology are shown in Fig. 18. Note that, the loss is equalized among all the resonators, and as a result, two imaginary and three complex coupling coefficients appear in the coupling matrix. One subsequently applies the proposed decomposition technique to the complex coupling matrix in Fig. 18(a), leading to five sub-matrices corresponding to five resistive connections, as shown in Fig. 19, and one residue matrix corresponding to the conventional coupling matrix without complex coupling values, as shown in Fig. 20(a). As expected, the residue coupling matrix has a uniform loss distribution among all the resonators. All the resistive connection sub-matrices are further combined together to form a single resistive connection matrix

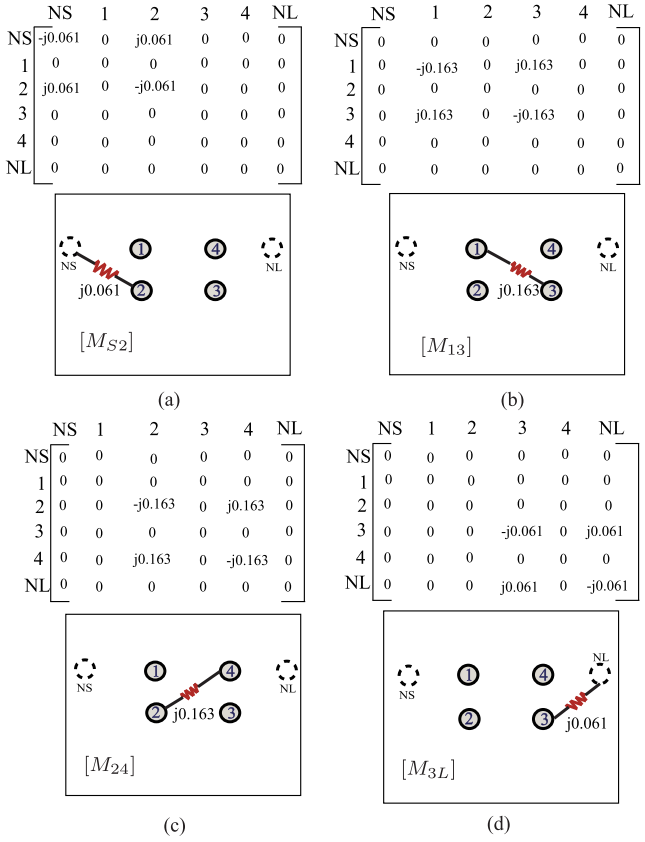

FIGURE 15. Four resistive connection sub-matrices decomposed from the complex coupling matrix of Fig. 14(a).

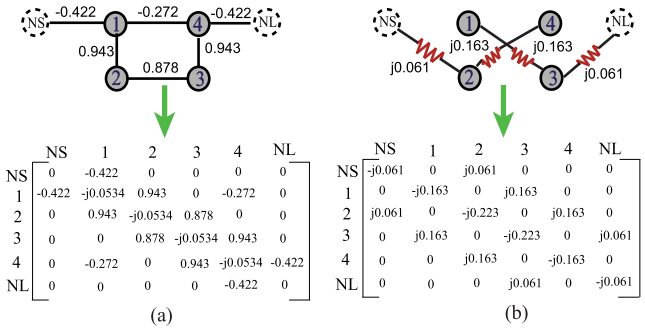

FIGURE 16. (a) Residue coupling matrix $[M]_{conv}$ and (b) resistive connection matrix $[M]_{resistor}$ after the decomposition of Fig. 14(a).

TABLE 3. Synthesized polynomials of example III.

$E(s)$	$s^3 + (2.2488 - j0.149)s^2$ $+(3.0586 + j0.1686)s + 1.8516 + j0.756$
$P(s)$	$j0.5s - 1$
$F_{11}(s) = F_{22}(s)$	$0.5s^3 - j0.0745s^2 + 0.265s - 0.0035$

and topology, as shown in Fig. 20(b). Finally, one has two matrices in Fig. 20, one corresponding to the conventional coupling matrix and the other corresponding to the resistive connection matrix.

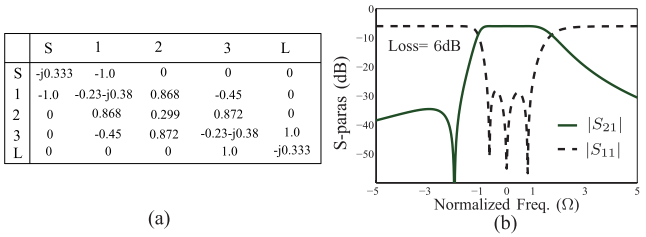

FIGURE 17. (a) Coupling matrix and (b) magnitude responses of example III before loss equalization.

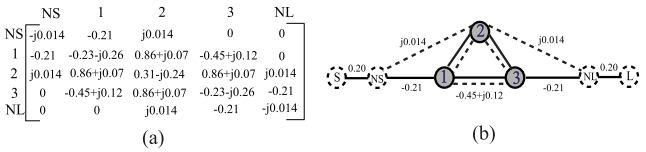

FIGURE 18. (a) Coupling matrix and (b) topology of example III after loss equalization with input/output couplings of $M_{S,NS} = M_{L,NL} = 0.205$.

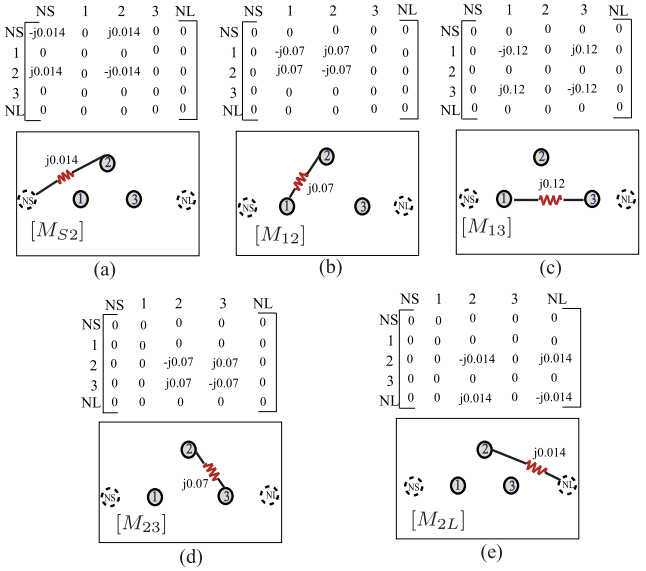

FIGURE 19. Five resistive connection sub-matrices decomposed from the complex coupling matrix of Fig. 18(a).

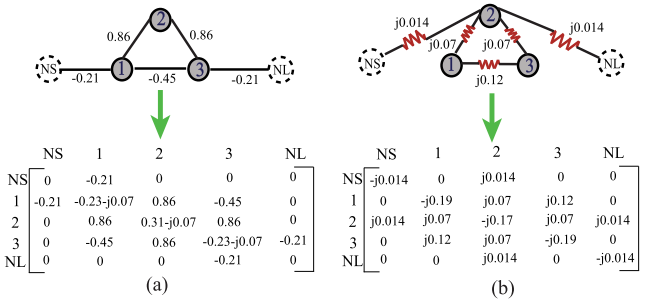

FIGURE 20. (a) Residue coupling matrix $[M]_{conv}$ and (b) resistive connection matrix $[M]_{resistor}$ after the decomposition of Fig. 18(a).

In summary, all the three illustrative examples achieve the expected results, which finally validate the proposed decomposition technique and loss equalization strategy.

VI. EXPERIMENTAL VALIDATION

To further experimentally validate the proposed technique, we physically implement the bandpass version of example I in Fig. 10 having a loss of 8.5 dB. The specified frequency range centers at 0.925 GHz with a bandwidth of 85 MHz. Roger RT Duroid-6010 (tanD=0.0023) substrate with a relative dielectric constant of $\epsilon_r = 10.2$ and thickness of 1.27 mm is used for implementation.

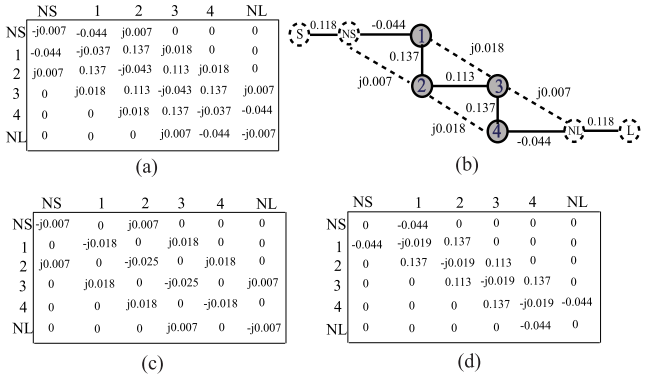

FIGURE 21. Bandpass version of example I: (a) coupling matrix with input/output couplings $M_{S,NS} = M_{L,NL} = 0.1183$, (b) coupling topology, (c) resistive connection matrix $[M]_{\text{resistor}}$, and (d) residual matrix $[M]_{\text{conv}}$.

The synthesized bandpass coupling matrix, topology, decomposed resistive connection matrix and residue conventional matrix are shown in Fig. 21. According to the calculation approach in [4], the diagonal entries of Fig. 21(d), $-j0.019$, correspond to unloaded quality factors of 230, which are implemented by 1.2 mm wide half-wavelength transmission line resonators. All the other real coupling coefficients in off-diagonal entries of Fig. 21(d) are implemented by coupled-line structures and are extracted using the conventional technique in [4]. Once the conventional coupling matrix $[M]_{\text{conv}}$ (Fig. 21(d)) is implemented by physical structures, we connect resistors between resonators according to the resistive connection matrix in Fig. 21(c) where all values are calculated according to (4).

Once all initial dimensions are obtained, a full-wave EM simulations have been carried out using Advanced Design System (ADS). Global full-wave optimization is performed to fine tune all parameters including resistors. Fig. 22 shows the fabricated prototype with optimized parameters. Two shorted shunt stubs are used at both ports to achieve the desired input/output coupling ($M_{S,NS}$ and $M_{L,NL}$) values of 0.1183. The final scattering parameters are measured by using two-port measurement with a Vector Network Analyzer (VNA). Fig. 23 shows the measured transmission and reflection magnitude responses in comparison with the ones calculated from the synthesized coupling matrix of Fig. 21(a). The measured results agree well with the synthesized ones, despite a slight deviation probably due to the tolerances brought by lumped resistors and fabrication.

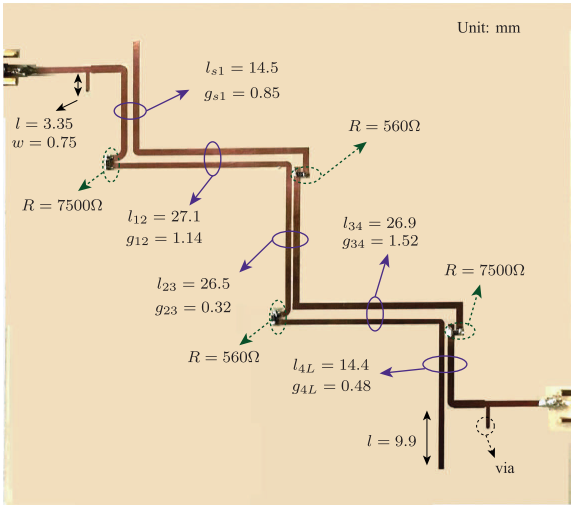

FIGURE 22. Fabricated prototype of the lossy filter in Fig. 21.

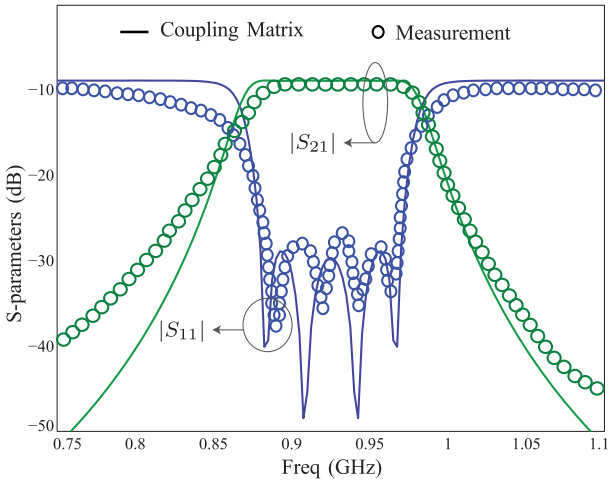

FIGURE 23. Measured transmission and reflection responses of the fabricated prototype in Fig. 22.

VII. DISCUSSION

We have demonstrated that using series resistor as fundamental block accompanied by proposed CM decomposition for all passive realization of highly lossy filters results easy tuning with perfect inband matching responses. We can easily compare this proposed technique with some of the existing lossy filter design techniques with their responses to prove the effectiveness of the proposed design method. Most of the existing works realized lossy couplings by lumped resistor coupled to resonators via high impedance transmission lines as shown in Fig. 6(b) in Sec. II-B. For instance [13], [15], realized lossy cross-couplings using Fig. 6(b) technique while [25] used nonuniform Q resonators to design lossy filters. In [25], as expected inband measured results significantly deviate from simulated one which suggest such implementation leads to degradation in filter performances. Similarly, previous lossy filter work in [13] also suffer from

mismatch issues. Because for every lossy coupling coefficients, it introduces many components (as shown in Fig. 6(b)) as a result, not only tuning become difficult but network becomes more sensitive to tolerances which leads to large inband imperfection. SIW based lossy filters very often deal with design complexities related to dissipative couplings [20]. Recently multi-layer PCB technology based lossy filters [21] were designed using conventional RCC structures for lossy cross-couplings. In this work, we used simple microstrip technology to design highly lossy filters by modifying ideal inverters as fundamental passive resistor blocks. Proposed method can overcome all these existing problems as it simplify lossy cross-coupling realization by a series resistor. Also tuning become much easier which results better inband S-parameters matching as compared to these existing works. As expected proposed designed are less sensitive to tolerances since it uses minimal components which is also clear from measured responses as depicted in Fig. 23 where some out-of-band deviation are visible but inband mismatches are negligible. Therefore this work proposes superior design methodology as compare to all other existing works.

VIII. CONCLUSION

Lossy filters are useful for satellite communication systems. Such filters are often deal with complex coupling matrices. A decomposition technique for the realization of complex coupling matrix has been presented. A new building block called resistive connection has been introduced to the coupling matrix. Proposed method is very useful for complete passive realization of lossy filters. This technique is versatile as it can deals with any coupling topology. Three numerical examples and one experimental validation were provided. The results finally validated the proposed technique.

REFERENCES

[1] A. E. Atia and A. E. Williams, "Narrow-bandpass waveguide filters," *IEEE Trans. Microw. Theory Techn.*, vol. 20, no. 4, pp. 258–265, Apr. 1972.
[2] R. J. Cameron, "Advanced coupling matrix synthesis techniques for microwave filters," *IEEE Trans. Microw. Theory Techn.*, vol. 51, no. 1, pp. 1–10, Jul. 2003.
[3] I. M. Filanovsky, "Property of rational functions related to band-pass transformation with application to symmetric filters design," *IEEE Trans. Circuits Syst. I, Reg. Papers*, vol. 63, no. 12, pp. 2112–2119, Dec. 2016.
[4] R. Cameron, C. Kudsia, and R. Mansour, *Microwave Filters for Communication Systems: Fundamentals, Design, and Applications*, vol. 1. Hoboken, NJ, USA: Wiley, 2007.
[5] F. Xiao, "Direct synthesis of general Chebyshev bandpass filters in the bandpass domain," *IEEE Trans. Circuits Syst. I, Reg. Papers*, vol. 61, no. 8, pp. 2411–2421, Aug. 2014.
[6] J.-X. Xu and X. Y. Zhang, "Single- and dual-band LTCC filtering switch with high isolation based on coupling control," *IEEE Trans. Ind. Electron.*, vol. 64, no. 4, pp. 3137–3146, Apr. 2017.
[7] M. Yu, W.-C. Tang, A. Malarky, V. Dokas, R. Cameron, and Y. Wang, "Predistortion technique for cross-coupled filters and its application to satellite communication systems," *IEEE Trans. Microw. Theory Techn.*, vol. 51, no. 12, pp. 2505–2515, Dec. 2003.
[8] A. C. Guyette, I. C. Hunter, and R. D. Pollard, "A new class of selective filters using low-Q components suitable for MMIC implementation," in *IEEE MTT-S Int. Microw. Symp. Dig.*, vol. 3, Jun. 2004, pp. 1959–1962.
[9] B. S. Senior, I. C. Hunter, and J. D. Rhodes, "Synthesis of lossy filters," in *Proc. 32nd Eur. Microw. Conf.*, Sep. 2002, pp. 1–4.
[10] L. Szydlowski, A. Lamecki, and M. Mrozowski, "Synthesis of coupled-lossy resonator filters," *IEEE Microw. Wireless Compon. Lett.*, vol. 20, no. 7, pp. 366–368, Jul. 2010.
[11] L. Szydlowski, A. Lamecki, and M. Mrozowski, "On the synthesis of coupled-lossy resonator filters with unloaded quality factor control," in *Proc. 18th Int. Conf. Microw., Radar Wireless Commun.*, Jun. 2010, pp. 1–3.
[12] L. Szydlowski, A. Lamecki, and M. Mrozowski, "Design of microwave lossy filter based on substrate integrated waveguide (SIW)," *IEEE Microw. Wireless Compon. Lett.*, vol. 21, no. 5, pp. 249–251, May 2011.
[13] A. C. Guyette, I. C. Hunter, and R. D. Pollard, "The design of microwave bandpass filters using resonators with nonuniform *Q*," *IEEE Trans. Microw. Theory Techn.*, vol. 54, no. 11, pp. 3914–3922, Nov. 2006.
[14] A. A. Müller, A. Moldoveanu, V. Asavei, E. Sanabria-Codesal, and J. F. Favennec, "Lossy coupling matrix filter synthesis based on hyperbolic reflections," in *IEEE MTT-S Int. Microw. Symp. Dig.*, May 2016, pp. 1–4.
[15] V. Miraftab and M. Yu, "Generalized lossy microwave filter coupling matrix synthesis and design using mixed technologies," *IEEE Trans. Microw. Theory Techn.*, vol. 56, no. 12, pp. 3016–3027, Dec. 2008.
[16] V. Miraftab and M. Yu, "Advanced coupling matrix and admittance function synthesis techniques for dissipative microwave filters," *IEEE Trans. Microw. Theory Techn.*, vol. 57, no. 10, pp. 2429–2438, Oct. 2009.
[17] M. Żukociński and A. Abramowicz, "Lossy inverters and their influence on coupled resonator filter characteristics," in *Proc. IEEE Int. Conf. Microw., Commun., Antennas Electron. Syst. (COMCAS)*, Oct. 2013, pp. 1–5.
[18] A. Basti, A. Périgaud, S. Bila, S. Verdeyme, L. Estagerie, and H. Leblond, "Design of microstrip lossy filters for receivers in satellite transponders," *IEEE Trans. Microw. Theory Techn.*, vol. 62, no. 9, pp. 2014–2024, Sep. 2014.
[19] L.-F. Qiu, L.-S. Wu, W.-Y. Yin, and J.-F. Mao, "Lossy filter with uniform Q-factors by optimization method," in *Proc. Asia–Pacific Microw. Conf.*, Nov. 2014, pp. 1300–1302.
[20] L.-F. Qiu, L.-S. Wu, B. Xie, W.-Y. Yin, and J.-F. Mao, "Substrate integrated waveguide filter with flat passband based on complex couplings," *IEEE Microw. Wireless Compon. Lett.*, vol. 28, no. 6, pp. 494–496, Jun. 2018.
[21] J. Ni, J. Hong, and P. M. Iglesias, "Compact microstrip if lossy filter with ultra-wide stopband," *IEEE Trans. Microw. Theory Techn.*, vol. 66, no. 10, pp. 4520–4527, Oct. 2018.
[22] R. Das, Q. Zhang, and H. Liu, "Lossy coupling matrix synthesis approach for the realization of negative group delay response," *IEEE Access*, vol. 6, pp. 1916–1926, 2017.
[23] L. Szydlowski, N. Leszczynska, and M. Mrozowski, "Generalized chebyshev bandpass filters with frequency-dependent couplings based on stubs," *IEEE Trans. Microw. Theory Techn.*, vol. 61, no. 10, pp. 3601–3612, Oct. 2013.
[24] R. Das, Q. Zhang, A. Kandwal, H. Liu, and Y. Chen, "Computer-aided tuning of highly lossy microwave filters using complex coupling matrix decomposition and extraction," *IEEE Access*, vol. 6, pp. 57172–57179, 2018.
[25] M. Meng and I. C. Hunter, "The design of parallel connected filter networks with non-uniform Q resonators," in *IEEE MTT-S Int. Microw. Symp. Dig.*, Jun. 2012, pp. 1–3.

RANJAN DAS (S'16) received the B.E. degree in electronics and instrumentation engineering from Jadavpur University, India, and the master's and Ph.D. degrees from the Electrical Engineering Department, IIT Bombay, Mumbai, India, in 2018. Since 2016, he has been with the Electronics and Electrical Engineering Department, South University of Science and Technology of China, Shenzhen, China, as a Visiting Researcher. His major research interests include reconfigurable microwave components designs, filter synthesis, and real-time analog signal processing of microwave signals.

QINGFENG ZHANG (S'07–M'11–SM'15) received the B.E. degree in electrical engineering from the University of Science and Technology of China, Hefei, China, in 2007, and the Ph.D. degree in electrical engineering from Nanyang Technological University, Singapore, in 2011. From 2011 to 2013, he was a Post-Doctoral Fellow with the Poly-Grames Research Center, École Polytechnique de Montréal, Montreal, QC, Canada. Since 2013, he has been with the Southern University of Science and Technology, Shenzhen, China, as an Assistant Professor. He has authored/co-authored over 100 research papers. His research interests include emerging novel electromagnetics technologies and multidisplininary topics. He was a Publication Chair of the IEEE ICCS, in 2016, and a TPC Member of several international conferences, including the EUCAP 2015, APCAP 2015, and EUCAP 2017. He serves on the review board for several microwave journals. He has served as a Lead Guest Editor for the *International Journal of Antennas and Propagation*, from 2014 to 2015. He has been serving as an Associate Editor for the IEEE Access, since 2017. He received the Shenzhen Overseas High-Caliber Personnel Award, in 2014, the Guangdong Natural Science Funds for Distinguished Young Scholar Award, in 2015, the Shenzhen Nanshan Piloting Talents Award, in 2016, and the Guangdong Special Support Program for Top-Notch Young Talents Award, in 2017.

ABHISHEK KANDWAL (M'17) received the bachelor's and master's degrees (Hons.) from Himachal Pradesh University, India, in 2007 and 2009, respectively, and the Ph.D. degree in microstrip antennas from JUIT, Solan, India, in 2014. From 2014 to 2016, he was with the National Electronics and Computer Technology Centre, NSTDA, MOST, Thailand. From 2016 to 2018, he was a Post-Doctoral Fellow with the Electronics and Electrical Engineering Department, SUSTech, Shenzhen, China. He has also worked in DRDO (Defense), India and DTI (Defense), and Thailand projects on antennas, from 2010 to 2016. He is currently an Assistant Professor with the Institute of Biomedical and Health Engineering, SIAT, Chinese Academy of Sciences, Shenzhen, China, and is working on advanced antennas for microwave, mm-wave, and biomedical and health engineering. He has published over 40 papers in international journals and conferences such as the IEEE, Nature, Elsevier, and Wiley. His main research is focused on emerging novel electromagnetics technologies. He is a Life Member of the Material Research Society of India and a member of the International Frequency Sensor Association.

HAIWEN LIU (M'04–SM'13) received the B.S. degree in electronic system and the M.S. degree in radio physics from Wuhan University, Wuhan, China, in 1997 and 2000, respectively, and the Ph.D. degree in microwave engineering from Shanghai Jiao Tong University, Shanghai, China, in 2004. From 2004 to 2006, he was a Research Assistant Professor with Waseda University, Kitakyushu, Japan. From 2006 to 2007, he was a Research Fellow with Kiel University, Kiel, Germany, where he received the Alexander von Humboldt Research Fellowship. From 2007 to 2008, he was a Professor with the Institute of Optics and Electronics, Chengdu, China, where he was supported by the 100 Talents Program of the Chinese Academy of Sciences, Beijing, China. Since 2009, he has been a Chair Professor with East China Jiaotong University, Nanchang, China. From 2009 to 2017, he was with East China Jiaotong University. Since 2018, he has been with Xi'an Jiaotong University, Xi'an, China, as a Professor. He has authored over 100 papers in international and domestic journals and conferences. His current research interests include electromagnetic modeling of high-temperature superconducting circuits, radio frequency and microwave passive circuits and systems, synthesis theory and practices of microwave filters and devices, antennas for wireless terminals, and radar systems.